

Received June 29, 2019, accepted August 19, 2019, date of publication August 26, 2019, date of current version September 12, 2019.

Digital Object Identifier 10.1109/ACCESS.2019.2937628

Millimeter Wave Time-Varying Channel Estimation via Exploiting Block-Sparse and Low-Rank Structures

LONG CHENG^{ID1,2}, GUANGRONG YUE^{ID1}, (Member, IEEE), DAIZHONG YU¹, YUEYUE LIANG³, AND SHAOQIAN LI¹, (Fellow, IEEE)

¹National Key Laboratory of Science and Technology on Communications, University of Electronic Science and Technology of China, Chengdu 611731, China

²Science and Technology on Information Transmission and Dissemination in Communication Networks Laboratory, Shijiazhuang 050081, China

³School of Electronic Engineering, Beijing University of Posts and Telecommunications, Beijing 100876, China

Corresponding author: Guangrong Yue (yuegr@uestc.edu.cn)

This work was supported in part by the National Natural Science Foundation of China under Grant 61831004, in part by the Defense Industrial Technology Development Program under Grant JCKY2016204A603, in part by the ITDCN Open Program under Grant 614210402070517, and in part by the National Defense Science and Technology Innovation Special Zone Project of China.

ABSTRACT The acquisition of channel state information is crucial in millimeter wave (mmWave) massive multiple-input multiple-output (MIMO) systems. However, the previous studies for mmWave channel estimation only focus on the conventional static channel model without considering the Doppler shifts in a time-varying scenario. Since the variations of angles are much shorter than that of path gains, the mmWave time-varying channel has block-sparse and low-rank characteristics. In this paper, we show that the block sparsity, along with the low-rank structure, can be utilized to extract the Doppler shifts and other channel parameters. Specially, to effectively exploit the block-sparse and low-rank structures, a two-stage method is proposed for mmWave time-varying channel estimation. In the first stage, we formulate a block-sparse signal recovery problem for AoAs/AoDs estimation, and we develop a block orthogonal matching pursuit (BOMP) algorithm to estimate the AoAs/AoDs. In the second stage, we formulate a low-rank tensor due to the low-rank structure of time-varying channels, and based on the results of the first stage, a CANDECOMP/PARAFAC (CP) decomposition-based algorithm is proposed to estimate the Doppler shifts and path gains. In addition, in order to compare with conventional tensor decomposition-based algorithms, two tensor decomposition-based time-varying channel estimation algorithms are proposed. Simulation results demonstrate that the proposed channel estimation algorithm outperforms the conventional compressed sensing-based algorithms and the tensor decomposition-based algorithms, and the proposed algorithm remains close to the Cramér-Rao Lower Bound (CRLB) even in the low SNR region with the priori knowledge of AoAs/AoDs.

INDEX TERMS Time-varying channel estimation, block-sparse, low-rank, compressed sensing, tensor decomposition.

I. INTRODUCTION

Global mobile system capacity will increase dramatically in the coming years, driven by ultra high definition videos, smart vehicular communications, and virtual reality etc. The demands for high data rate transmission will reach $1000 \times$ over the next decade, as predicted in [1]. Millimeter-wave (mmWave) (30-300GHz) techniques, which can easily deploy large-scale antenna arrays and potentially offer

The associate editor coordinating the review of this article and approving it for publication was Vittorio Degli-Esposti.

Gbps transmission rate by exploiting the large communication bandwidth [2], have been considered as new radio transmissions to meet the large data demand for future wireless communications [3]. For example, a maximum data rate of 20Gbs is achievable under the ambit of the IEEE 802.11ay standard for 60GHz indoor communications [4]. However, the transmission in the mmWave frequency band may exhibit the higher path loss compared to that in the lower frequency bands [5]. Fortunately, large antenna arrays can be utilized to provide beamforming gain to compensate the signal energy attenuation [6].

Massive multiple-input multiple output (MIMO) operating in mmWave leads to challenges of designing channel estimation algorithms [7]. Recently, by leveraging the sparse nature of mmWave channels, the channel estimation is formulated as a line sparse recovery problem. To solve this problem, compressed sensing (CS) has been widely used to achieve substantial training overhead reduction [8]–[12]. In particular, the authors of [8] have developed an alternative CS-based open-loop channel estimator for mmWave hybrid MIMO systems. To reduce the complexity of the conventional CS methods, a two-stage CS method has been proposed in [9]. Furthermore, although conventional CS-based methods assume that the estimated angles lie in the pre-specified grid points in angle domain, the actual angle of arrivals/departures (AoAs/AoDs) do not necessarily locate in the grid. Thus, the assumption of on-grid angles results in a grid mismatch problem, which leads to deteriorated performance for channel estimation. To mitigate the performance degradation, some super-resolution channel estimation algorithms have been proposed in [10], [11]. In addition to the sparse scattering nature, mmWave channels may exhibit a low-rank structure. Specially, the received signal can be expressed as a low-rank tensor. Moreover, some tensor decomposition-based methods [13], [14] are recently proposed to estimate all the channel parameters including AoAs/AoDs, time delays, and path gains, and it has been shown that these methods present distinguish advantages over the conventional CS-based algorithms.

However, most of the existing studies [8]–[14] only focus on the investigation of channel estimation algorithms in the presence of static mmWave channel model, without considering the Doppler shifts in the time-varying channel model. In fact, mmWave may play a important role in providing high date transmission for the future high mobility scenarios, such as the high speed wearable networks [5], the autonomous vehicular communications [15], the unmanned aerial vehicles (UAVs) communications [16], and high speed trains (HSTs) [17]. Specially, it is shown that the speed of HST can reach 500km/h, where the mmWave channel of this scenario will change much more rapidly compared to the conventional MIMO channel. The study in [18] has proposed an adaptive estimation (AAE) algorithm for the time-varying mmWave channel. However, it suffers from the overhead transmission from the receiver to the transmitter. This motivates us to investigate efficient channel estimation algorithms in time-varying mmWave massive MIMO systems.

In this work, a novel channel estimation algorithm by exploiting the block-sparse and low-rank characteristics is proposed for time-varying mmWave massive MIMO systems.

The main contributions of our work are summarized as follows.

- 1) A two-stage channel estimation scheme is proposed for the mmWave time-varying channel. Since the variations of angles are much shorter than that of path gains, the mmWave time-varying channel represents block sparse characteristic. In addition to the block

sparsity, mmWave time-varying channels may exhibit low-rank structure. Thus, the received data can be modeled as a third-order low-rank tensor. To effectively exploit the block-sparse and low-rank characteristics, a two-stage channel estimation method is proposed. In the first stage, we formulate a block-sparse signal recovery problem for AoAs/AoDs estimation, and we develop a block orthogonal matching pursuit (BOMP) algorithm to estimate the AoAs/AoDs. In the second stage, we formulate a low-rank tensor due to the low-rank structure of time-varying channels, and based on the results of the first stage, we propose a CANDECOMP/PARAFAC (CP) decomposition-based algorithm to estimate the Doppler shifts and path gains.

- 2) For comparison with the conventional tensor decomposition-based algorithms, two CP decomposition-based channel estimation schemes are proposed for the mmWave time-varying channel estimation. Firstly, through analysis, we conclude that the dimension extension method proposed in this paper cannot satisfy the uniqueness condition of CP decomposition. Then, exploiting the approximation in [19], a simply extended CP decomposition-based algorithm is proposed. Secondly, in order to estimate the channel gains and Doppler shifts effectively, an improved CP decomposition-based algorithm is proposed
- 3) We derive the Cramér-Rao Lower Bound (CRLB) for the proposed scheme and provide the computational complexity. Moreover, the simulation results show that the proposed channel estimation algorithm outperforms the conventional compressed sensing-based algorithms and the tensor decomposition-based algorithms. In addition, simulation results also show that the proposed scheme remains close to the CRLBs even in the low SNR region with the priori knowledge of AoAs/AoDs.

The rest of the paper is organized as follows. Section II and III introduce the system model and the block-sparse and low-rank characteristics of the mmWave time-varying channel. In Section IV, we propose a two-stage channel estimation method. Two CP decomposition-based time-varying channel estimation methods are proposed in Section V. The analysis of the proposed algorithm is provided in Section VI. The simulation results are given in Section VII. Finally, Section VIII draws a conclusion.

Notation: The matrices and vectors are denoted in bold. Symbols $(\cdot)^*$, $(\cdot)^\dagger$, $(\cdot)^H$, $(\cdot)^T$, $\|\cdot\|_F$ denote its conjugate, pseudo-inverse, conjugate transpose, transpose, and Frobenius norm, respectively. The $K \times K$ identity matrix is given by I_K . $\boldsymbol{\kappa}_{(n)}$ is the mode- n unfolding of the tensor $\boldsymbol{\kappa}$. The outer product of two vectors is given by $\mathbf{a} \circ \mathbf{b}$. $\mathbf{A} \odot \mathbf{B}$ is the Khatri-Rao product of matrices \mathbf{A} and \mathbf{B} .

II. SYSTEM MODEL

Consider a typical point-to-point narrowband uplink mmWave massive MIMO system shown in Fig. 1, where

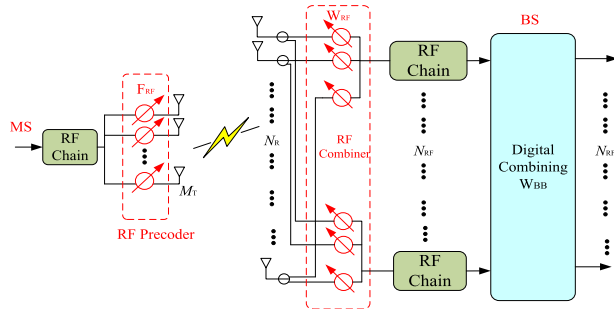


FIGURE 1. A block diagram of the uplink mmWave MIMO architecture that employs hybrid analog/digital precoding.

the base station (BS) is equipped with N_R antennas and N_{RF} radio frequency (RF) chains, where $N_{RF} \ll N_R$ and the mobile station (MS) employs M_T antennas and a single RF chain [20].

For a practical mmWave massive MIMO system with hybrid precoding, the MS first modulates the baseband data symbols via an analog precoder $\mathbf{F}_{RF} \in \mathbb{C}^{M_T \times 1}$. Hence, signal vector transmitted by the MS at the time instant t can be expressed as (see, e.g. [4])

$$\mathbf{f}(t) = \mathbf{F}_{RF}(t)s(t), \quad (1)$$

where $s(t)$ denotes the transmitted symbol and without loss of generality, we set $s(t) = 1$. Since \mathbf{F}_{RF} is implemented using analog phase shifters, its entries are of constant modulus, where $|\mathbf{f}_m(t)| = 1 (m = 1, \dots, M_T)$. Then, at the BS, the received signal at the time instant t is combined with a RF combiner $\mathbf{W}_{RF}(t) \in \mathbb{C}^{N_R \times N_{RF}}$ and followed by a digital combiner $\mathbf{W}_{BB}(t) \in \mathbb{C}^{N_{RF} \times N_{RF}}$, it yields

$$\begin{aligned} \mathbf{y}(t) &= (\mathbf{W}_{RF}(t)\mathbf{W}_{BB}(t))^H \mathbf{H}(t) \mathbf{F}_{RF}(t)s(t) + \mathbf{N}(t) \\ &= \mathbf{w}^H(t)\mathbf{H}(t)\mathbf{f}(t) + \mathbf{N}(t), \end{aligned} \quad (2)$$

where $\mathbf{w}(t) \triangleq \mathbf{W}_{RF}(t)\mathbf{W}_{BB}(t)$ denotes the combiner at the t -th instant, $\mathbf{y}(t) \in \mathbb{C}^{N_{RF} \times 1}$ is the received signal, and $\mathbf{N}(t) \sim \mathcal{CN}(0, 1)$ denotes the additive white Gaussian noise vector. In addition, the elements of defined combiner $\mathbf{w}(t)$ have the similar constant modulus to precoder $\mathbf{f}(t)$ as follows

$$|\mathbf{w}_n(t)| = 1 (n = 1, \dots, N_R). \quad (3)$$

Since the mmWave channel exhibits limited scattering characteristics, we consider a geometric mmWave channel model with L scatters between the MS and the BS. Furthermore, to incorporate the Doppler shifts with the conventional mmWave channel, the time-varying channel at the t -th instant can be expressed as [21]

$$\mathbf{H}(t) = \sum_{l=1}^L a_l(t) \boldsymbol{\alpha}_{BS}(\theta_l(t)) \boldsymbol{\alpha}_{MS}^H(\varphi_l(t)) e^{j2\pi f_l T_s t}, \quad (4)$$

where L denotes the number of scatter paths and $a_l(t) \sim \mathcal{CN}(0, 1)$ denotes the complex gain. $\boldsymbol{\alpha}_{BS}(\theta_l(t)) \in \mathbb{C}^{N_R \times 1}$ and $\boldsymbol{\alpha}_{MS}(\varphi_l(t)) \in \mathbb{C}^{M_T \times 1}$ are the array response vectors associated with the BS and MS, respectively. $\theta_l(t), \varphi_l(t) \in [0, 2\pi]$

denote the angles of arrival and departure (AoAs/AoDs) of the l -th path, respectively. Furthermore, for the time-varying channel parameters, f_l and T_s are the Doppler shift and sampling period, respectively. As we consider the uniform linear array (ULA) to be used in our system, then the steering vectors can be expressed as

$$\begin{aligned} \boldsymbol{\alpha}_{BS}(\theta_l(t)) &= \frac{1}{\sqrt{N_R}} [1, \dots, e^{j(N_R-1)\frac{2\pi}{\lambda}d \sin(\theta_l(t))}]^T, \\ \boldsymbol{\alpha}_{MS}(\varphi_l(t)) &= \frac{1}{\sqrt{M_T}} [1, \dots, e^{j(M_T-1)\frac{2\pi}{\lambda}d \sin(\varphi_l(t))}]^T, \end{aligned} \quad (5)$$

where λ denotes the signal wave length, and we set the distance $d = \lambda/2$.

III. BLOCK-SPARSE AND LOW-RANK PRESENTATIONS OF TIME-VARYING mmWAVE CHANNELS

In this section, we first simplify the mmWave channel time-varying channel model based on a reasonable assumption. Then, based on the novel time-varying channel, the block-sparse and low-rank characteristics are discussed.

A. TIME-VARYING CHANNEL MODEL SIMPLIFICATION

Since the AoAs/AoDs and complex gains vary slowly in the high-mobility scenarios [18], [22], [23], it is reasonable to make the same assumption presented in [18], [23] that the time-varying channel parameters $\theta_l(t)$, $\varphi_l(t)$ and $a_l(t)$ remain constant during a training frame. Therefore, in a training frame, the mathematical expressions of those time-varying parameters are as follows

$$\theta_l(t) = \theta_l, \quad \varphi_l(t) = \varphi_l, \quad a_l(t) = a_l. \quad (6)$$

Then, the mmWave time-varying channel model can be rewritten as follows

$$\begin{aligned} \mathbf{H}(t) &= \sum_{l=1}^L a_l \boldsymbol{\alpha}_{BS}(\theta_l) \boldsymbol{\alpha}_{MS}^H(\varphi_l) e^{j2\pi f_l T_s t} \\ &= \sum_{l=1}^L \rho_l(t) \boldsymbol{\alpha}_{BS}(\theta_l) \boldsymbol{\alpha}_{MS}^H(\varphi_l), \end{aligned} \quad (7)$$

where $\rho_l(t)$ denotes the novel time-varying gain associated with the Doppler shift. In particular, the path gain $\rho_l(t)$ varies with time even in a training frame. Then, in the next subsections, the special characteristics of the channel model will be discussed.

B. BLOCK-SPARSE PRESENTATION

In order to effectively reflect the sparsity of mmWave channel, we first express the channel model in the beamspace as follows

$$\mathbf{H}(t) = \mathbf{A}_{BS} \mathbf{H}_v(t) \mathbf{A}_{MS}^H, \quad (8)$$

where $\mathbf{H}_v(t) \in \mathbb{C}^{N_1 \times N_2}$ denotes the beamspace channel matrix, $\mathbf{A}_{BS} \in \mathbb{C}^{N_R \times N_1}$ and $\mathbf{A}_{MS} \in \mathbb{C}^{M_T \times N_2}$ denote the overcomplete dictionary matrices (i.e., $N_1 \geq N_R$, $N_2 \geq M_T$) consisting of the steering vectors corresponding with the pre-discretized

AoAs and AoDs, respectively. For example, the n -th column in \mathbf{A}_{BS} can be expressed as

$$\mathbf{A}_{\text{BS}}^{:,n} = \frac{1}{\sqrt{N_{\text{R}}}} [1, e^{-j2\pi(n-1)/N_1}, \dots, e^{-j(N_{\text{R}}-1)2\pi(n-1)/N_1}]^T, \quad (9)$$

and the dictionary matrix \mathbf{A}_{MS} can be designed in a similar method.

The beamspace channel matrix $\mathbf{H}_v(t)$ is a sparse matrix with a few non-zero entries due to the sparse scattering characteristic. If all the true channel parameters lie in the dictionary matrix, the non-zero entries of $\mathbf{H}_v(t)$ are the channel path gains $\{a_l(t)\}$. However, because of the power leakage problem [10], the actual number of non-zero entries will be larger than the number of multipaths. Therefore, there exist $L_M \geq L$ non-zero elements in the beamspace channel matrix $\mathbf{H}_v(t)$.

By substituting (8) into (2), it yields

$$\begin{aligned} \mathbf{y}(t) &= [(\mathbf{A}_{\text{MS}}^H \mathbf{f}(t))^T \otimes (\mathbf{w}^H(t) \mathbf{A}_{\text{BS}})] \text{vec}(\mathbf{H}_v(t)) + \mathbf{N}(t) \\ &= (\mathbf{f}^H(t) \otimes \mathbf{w}^H(t)) (\mathbf{A}_{\text{MS}}^* \otimes \mathbf{A}_{\text{BS}}) \text{vec}(\mathbf{H}_v(t)) + \mathbf{N}(t) \\ &= \boldsymbol{\psi}(t) \text{vec}(\mathbf{H}_v(t)) + \mathbf{N}(t), \end{aligned} \quad (10)$$

where $\boldsymbol{\psi}(t) \triangleq (\mathbf{f}^H(t) \otimes \mathbf{w}^H(t)) (\mathbf{A}_{\text{MS}}^* \otimes \mathbf{A}_{\text{BS}}) \in \mathbb{C}^{N_{\text{RF}} \times N_1 N_2}$ can be viewed as a measurement matrix. Then, the estimation of the beamspace channel $\text{vec}(\mathbf{H}_v(t))$ now becomes a sparse recovery problem [7]–[12]. Specially, the conventional mmWave channel estimation algorithms assume that the channel is invariant in the training frame, thus only L_M non-zero entries need to be recovered. In particular, the positions of the non-zero entries denote the values of AoAs/AoDs. However, for the mmWave time-varying channel, the path gain $\rho_l(t)$ varies with time even in a training frame. Therefore, assuming M pilot signals, there are up to ML_M non-zero entries need to be recovered. Based on the basic theory of signal recovery, it is impossible to recover these entries accurately [24]. Specially, the received M measurements can be expressed as

$$\mathbf{y} = \begin{bmatrix} \boldsymbol{\psi}(1) & 0 & \cdots & 0 \\ 0 & \boldsymbol{\psi}(2) & \cdots & 0 \\ \vdots & \vdots & \ddots & \vdots \\ 0 & 0 & \cdots & \boldsymbol{\psi}(M) \end{bmatrix} \begin{bmatrix} \mathbf{h}(1) \\ \mathbf{h}(2) \\ \vdots \\ \mathbf{h}(M) \end{bmatrix} + \mathbf{N}, \quad (11)$$

where $\mathbf{y} = [\mathbf{y}^T(1), \dots, \mathbf{y}^T(M)]^T \in \mathbb{C}^{N_{\text{RF}} M \times 1}$ denotes the received signal vector, $\mathbf{N} \in \mathbb{C}^{N_{\text{RF}} M \times 1}$ denotes the additive white Gaussian noise vector and $\mathbf{h}(t) = \text{vec}(\mathbf{H}_v(t)) \in \mathbb{C}^{N_1 N_2 \times 1}$ denotes the beamspace channel at the t -th time instant. We denote $\mathbf{h} \triangleq [\mathbf{h}^T(1), \dots, \mathbf{h}^T(M)]^T \in \mathbb{C}^{M N_1 N_2 \times 1}$ as the received beamspace channel vector, which has ML_M non-zeros entries.

To solve the above problem, we first utilize the unique characteristic of mmWave time-varying channels to estimate AoAs/AoDs. In particular, since the AoAs/AoDs remain constant during a training frame, the received beamspace channel exhibits block-sparsity after some signal processing. Then the

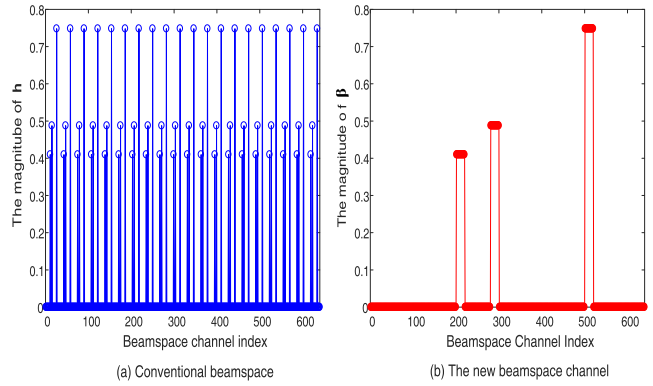


FIGURE 2. An illustration of a 3-path beamspace channel, where $M_T = 4$, $N_R = 8$.

received signals is formulated as

$$\begin{aligned} \mathbf{y} &= \underbrace{\begin{bmatrix} \boldsymbol{\psi}(1) & 0 & \cdots & 0 \\ 0 & \boldsymbol{\psi}(2) & \cdots & 0 \\ \vdots & \vdots & \ddots & \vdots \\ 0 & 0 & \cdots & \boldsymbol{\psi}(M) \end{bmatrix}}_{\Theta} \underbrace{\boldsymbol{\Pi} \boldsymbol{\Pi}^T}_{\Theta} \underbrace{\begin{bmatrix} \mathbf{h}(1) \\ \mathbf{h}(2) \\ \vdots \\ \mathbf{h}(M) \end{bmatrix}}_{\beta} + \mathbf{N} \\ &= \Theta \beta + \mathbf{N}, \end{aligned} \quad (12)$$

where $\Theta \in \mathbb{C}^{M N_{\text{RF}} \times M N_1 N_2}$ denotes the novel measurement matrix, $\beta \in \mathbb{C}^{M N_1 N_2 \times 1}$ is the novel beamspace channel, and $\boldsymbol{\Pi}$ denotes the permutation matrix which integrates the same position entry of the beamspace channel at different time instant. For example, Fig. 2 shows the difference between the original beamspace channel and the new beamspace channel, where all the AoAs/AoDs are assumed to be on grid. Therefore, the estimation of angles now becomes a block sparse signal recovery problem. By finding the locations of non-zero blocks, the AoAs/AoDs can be estimated. Then, to solve the problem, we can resort to some conventional block sparse algorithms, such as BOMP algorithm [25]. Since the locations of non-zero blocks are not related to the Doppler shifts, the above angle estimation algorithms are robust to different Doppler shifts.

C. LOW-RANK PRESENTATION

In addition to the block-sparsity, the time-varying mmWave channel may exhibit a meaningful low-rank tensor structure because of the time dimension. To better understand the tensor structure, we first provide some prerequisites about tensor decomposition, which can be found in [26], [27].

Definition 1 (Rank-one Tensor): The N -order tensor $\kappa \in \mathbb{C}^{I_1 \times I_2 \times \dots \times I_N}$ is rank-one if it can be expressed as

$$\kappa = \mathbf{a}_1 \circ \mathbf{a}_2 \circ \dots \circ \mathbf{a}_N, \quad (13)$$

where $\mathbf{a}_n \in \mathbb{C}^{I_n \times 1}$ ($n = 1, \dots, N$) denotes the factor vector.

Definition 2 (Tensor Rank):

The rank of a N -order tensor κ is defined as the smallest number of rank-one tensors that form tensor κ as their sum.

Definition 3 (CANDECOMP/PARAFAC Decomposition): The CANDECOMP/PARAFAC (CP) Decomposition, which is also known as canonical polyadic decomposition (CPD), factorizes a tensor into a sum of rank-one tensors. For example, the CP of a third-order tensor $\kappa \in \mathbb{C}^{I \times J \times K}$ has a form as

$$\kappa = \sum_{k=1}^K \mathbf{x}_k \circ \mathbf{y}_k \circ \mathbf{z}_k, \quad (14)$$

where K denotes the rank of tensor κ , $\mathbf{x}_k \in \mathbb{C}^{I \times 1}$ ($k = 1, \dots, K$) and likewise for \mathbf{y}_k and \mathbf{z}_k . Furthermore, the CP model can be rewritten as

$$\begin{aligned} \kappa &= [\mathbf{X}, \mathbf{Y}, \mathbf{Z}] \\ &= \sum_{k=1}^K \mathbf{x}_k \circ \mathbf{y}_k \circ \mathbf{z}_k, \end{aligned} \quad (15)$$

where $\mathbf{X} = [\mathbf{x}_1 \dots \mathbf{x}_K]$ denotes the factor matrix refer to the combination of the vectors and likewise for \mathbf{Y} and \mathbf{Z} . Furthermore, it is often assumed that the columns of \mathbf{X} , \mathbf{Y} , and \mathbf{Z} are normalized with the amplitudes absorbed into a new vector $\boldsymbol{\lambda} \in \mathbb{C}^{K \times 1}$, such as

$$\begin{aligned} \kappa &= [\boldsymbol{\lambda}; \mathbf{X}, \mathbf{Y}, \mathbf{Z}] \\ &= \sum_{k=1}^K \lambda_k \mathbf{x}_k \circ \mathbf{y}_k \circ \mathbf{z}_k. \end{aligned} \quad (16)$$

After the above necessary preparations, we start to construct the tensor model for mmWave time-varying MIMO channel. Based on (7), the time-varying channel at the t -th time instant can be developed as

$$\mathbf{H}(t) = \sum_{l=1}^L a_l e^{j2\pi f_l T_s t} \boldsymbol{\alpha}_{\text{BS}}(\theta_l) \circ \boldsymbol{\alpha}_{\text{MS}}^*(\varphi_l). \quad (17)$$

Then the time-varying channel for the M time instants can be expanded as

$$\begin{aligned} \boldsymbol{\chi} &= [\mathbf{a}; \mathbf{A}, \mathbf{B}, \mathbf{C}] \\ &= \sum_{l=1}^L \alpha_l \boldsymbol{\alpha}_{\text{BS}}(\theta_l) \circ \boldsymbol{\alpha}_{\text{MS}}^*(\varphi_l) \circ \boldsymbol{\beta}_l, \end{aligned} \quad (18)$$

where $\boldsymbol{\chi} \in \mathbb{C}^{N_R \times M_T \times M}$ denotes the third-order channel tensor whose three orders represent the AoA dimension, AoD dimension, and time dimension, respectively. $\mathbf{a} \in \mathbb{C}^{L \times 1}$ is the amplitude vector, $\boldsymbol{\beta}_l = [e^{j2\pi f_l T_s} \dots e^{j2\pi f_l T_s M}]^T \in \mathbb{C}^{M \times 1}$ and define

$$\mathbf{A} = [\boldsymbol{\alpha}_{\text{BS}}(\theta_1) \dots \boldsymbol{\alpha}_{\text{BS}}(\theta_L)] \in \mathbb{C}^{N_R \times L}, \quad (19)$$

$$\mathbf{B} = [\boldsymbol{\alpha}_{\text{MS}}^*(\varphi_1) \dots \boldsymbol{\alpha}_{\text{MS}}^*(\varphi_L)] \in \mathbb{C}^{M_T \times L}, \quad (20)$$

$$\mathbf{C} = [\boldsymbol{\beta}_1 \dots \boldsymbol{\beta}_L] \in \mathbb{C}^{M \times L}. \quad (21)$$

Based on the above derivation, it is clear to observe that the mmWave time-varying channel satisfies the form of CP decomposition when considering the time dimension. Furthermore, due to the sparse scattering nature of the mmWave time-varying channel, the number of paths, is usually very

small. Thus the channel tensor $\boldsymbol{\chi}$ has an intrinsic low-rank structure.

Our objective is to estimate the mmWave time-varying channel via utilizing the joint block sparse and low-rank structures. Since estimation of time-varying channel via utilizing revised BOMP algorithm [18], [23] and estimation of static channel via utilizing CP decomposition algorithm [13], [14] have been studied. However, there is much less research for cases where the time-varying channel is characterized by two structures simultaneously. In particular, how to utilize the two structures to improve the performance of time-varying channel estimation is of most concern. Thus, in the following section, a two-stage scheme is proposed to estimate time-varying channels by utilizing the two structures simultaneously.

IV. PROPOSED TWO-STAGE TIME-VARYING CHANNEL ESTIMATION ALGORITHM

In this section, we divide the proposed algorithm into two separate stages. In the first stage, we utilized the block-sparse structure to estimate the AoAs/AoDs of the mmWave time-varying channel. In the second stage, based on the estimated AoAs/AoDs, a CP decomposition-based method is developed to extract the path gains and the Doppler shifts by utilizing the low-rank structure. Through the above two stages, all the parameters of the time-varying channel are estimated, then the final channel can be recovered.

For the stage of AoAs/AoDs estimation, the MS employs M_1 pilot signals to estimate the time-varying channel, and at time instant t , the BS employs a combining matrix $\mathbf{w}_1(t) \in \mathbb{C}^{N_R \times N_{\text{RF}}}$ to receive signal and the MS employs a precoding vector $\mathbf{f}_1(t) \in \mathbb{C}^{M_T \times 1}$ as pilot signal. In particular, each entry of $\mathbf{w}_1(t)$ and $\mathbf{f}_1(t)$ can be chosen uniformly from a unit circle [14]. Then, similar to that described in the Section III-A, the received M_1 measurements can be expressed as

$$\mathbf{y} = \Theta \boldsymbol{\beta} + \mathbf{N}, \quad (22)$$

where $\mathbf{y} \in \mathbb{C}^{N_{\text{RF}} M_1 \times 1}$, $\Theta \in \mathbb{C}^{M_1 N_{\text{RF}} \times M_1 N_1 N_2}$, $\mathbf{N} \in \mathbb{C}^{N_{\text{RF}} M_1 \times 1}$, $\boldsymbol{\beta} \in \mathbb{C}^{M_1 N_1 N_2 \times 1}$ and all the above parameters are defined in Section III-A. Note that the beamspace channel $\boldsymbol{\beta}$ has a block-sparse structure and the locations of non-zero blocks denote the information of angles. Then a revised BOMP algorithm in [18] can be utilized to estimate the AoAs/AoDs and the number of non-zeros blocks, i.e., the number of paths \tilde{L} . Finally, as the locations of non-zero blocks are not related to the Doppler shifts, then this scheme is robust to different Doppler shifts.

For the second stage, the designs of pilot signal and combining matrix are different from that of the first stage. Specifically, the MS employs M_2 constant beamforming vectors \mathbf{f}_{MS} to detect the time-varying channel and the BS utilizes a constant combining matrix \mathbf{w}_2 to detect signals. In particular, the design of beamforming vector and combining matrix is similar to the design in the first stage. Then, different from the frame structure in the first stage, the received signal can be

written as

$$\mathbf{y}(t) = \mathbf{w}_2^H \mathbf{H}(t) \mathbf{f}_{\text{MS}} + \mathbf{N}(t), \quad (23)$$

where $\mathbf{w}_2 \in \mathbb{C}^{N_{\text{RF}} \times N_{\text{RF}}}$ and $\mathbf{f}_{\text{MS}} \in \mathbb{C}^{M_{\text{T}} \times 1}$. Then the received signal is multiplied by a precoding vector $\mathbf{f}_{\text{BS}} \in \mathbb{C}^{1 \times N_s}$ where each entry is chosen uniformly from a unit circle. The processed signal can be expressed as

$$\mathbf{R}(t) = \mathbf{w}_2^H \mathbf{H}(t) \mathbf{f}_2 + \mathbf{N}(t), \quad (24)$$

where $\mathbf{R}(t) = \mathbf{y}(t) \mathbf{f}_{\text{BS}} \in \mathbb{C}^{N_{\text{RF}} \times N_s}$, $\mathbf{f}_2 = \mathbf{f}_{\text{MS}} \mathbf{f}_{\text{BS}} \in \mathbb{C}^{M_{\text{T}} \times N_s}$ and $\mathbf{N}(t) \in \mathbb{C}^{N_{\text{RF}} \times N_s}$.

Furthermore, the processed signal can be rewritten as a form of a weighted sum of common set of rank-one outer products, such as

$$\begin{aligned} \mathbf{R}(t) &= \sum_{l=1}^L a_l e^{j2\pi f_l T_s t} \mathbf{w}_2^H \boldsymbol{\alpha}_{\text{BS}}(\theta_l) \boldsymbol{\alpha}_{\text{MS}}^H(\varphi_l) \mathbf{f}_2 + \mathbf{N}(t) \\ &= \sum_{l=1}^L a_l e^{j2\pi f_l T_s t} \overrightarrow{\boldsymbol{\alpha}}_{\text{BS}}(\theta_l) \circ \overrightarrow{\boldsymbol{\alpha}}_{\text{MS}}(\varphi_l) + \mathbf{N}(t), \end{aligned} \quad (25)$$

where $\overrightarrow{\boldsymbol{\alpha}}_{\text{BS}}(\theta_l) \triangleq \mathbf{w}_2^H \boldsymbol{\alpha}_{\text{BS}}(\theta_l)$, $\overrightarrow{\boldsymbol{\alpha}}_{\text{MS}}(\varphi_l) \triangleq \mathbf{f}_2^T \boldsymbol{\alpha}_{\text{MS}}^*(\varphi_l)$. And then, similar to what is discussed in Section III-C, the received data can be model as a low-rank tensor $\boldsymbol{\gamma} \in \mathbb{C}^{N_{\text{RF}} \times N_s \times M_2}$. Specially, the three modes represent the RF chain of BS, the extended dimension, the time instant, respectively. Therefore, the tensor $\boldsymbol{\gamma}$ can be rewritten as a form of CP decomposition, i.e.

$$\begin{aligned} \boldsymbol{\gamma} &= \sum_{l=1}^L a_l \overrightarrow{\boldsymbol{\alpha}}_{\text{BS}}(\theta_l) \circ \overrightarrow{\boldsymbol{\alpha}}_{\text{MS}}(\varphi_l) \circ \boldsymbol{\beta}_l + \mathbf{N} \\ &= [\mathbf{a}, \overrightarrow{\mathbf{A}}, \overrightarrow{\mathbf{B}}, \mathbf{C}] + \mathbf{N}, \end{aligned} \quad (26)$$

where

$$\overrightarrow{\mathbf{A}} = [\overrightarrow{\boldsymbol{\alpha}}_{\text{BS}}(\theta_1) \cdots \overrightarrow{\boldsymbol{\alpha}}_{\text{BS}}(\theta_L)] \in \mathbb{C}^{N_{\text{RF}} \times L}, \quad (27)$$

$$\overrightarrow{\mathbf{B}} = [\overrightarrow{\boldsymbol{\alpha}}_{\text{MS}}(\varphi_1) \cdots \overrightarrow{\boldsymbol{\alpha}}_{\text{MS}}(\varphi_L)] \in \mathbb{C}^{N_s \times L}. \quad (28)$$

To obtain the three estimated factor matrices $\widetilde{\mathbf{A}}$, $\widetilde{\mathbf{B}}$, $\widetilde{\mathbf{C}}$, alternating lease square (ALS) method is always exploited by conventional CP decomposition-based algorithms [13], [26], [27]. However, these algorithms need to design unique precoding and combing matrices to ensure the uniqueness of CP decomposition. Meanwhile, these algorithms are only suitable for static mmWave channel estimation. In our two-stage scheme, by utilizing the block-sparse structure of mmWave time-varying channels, the AoAs/AoDs can be obtained. Then, a novel CP decomposition method is proposed by utilizing the basic property of CP decomposition. Specially, regardless of the uniqueness condition of the CP decomposition, the equality of noiseless $\boldsymbol{\gamma}$ is always held as follows [27]

$$\boldsymbol{\gamma}_{(3)} = \mathbf{C} \mathbf{A} (\overrightarrow{\mathbf{B}} \odot \overrightarrow{\mathbf{A}})^T, \quad (29)$$

where $\mathbf{A} = \text{diag}(\mathbf{a})$. Therefore, based on the estimated angles, the estimated factor matrix $\widetilde{\mathbf{E}} \triangleq \widetilde{\mathbf{C}} \widetilde{\Lambda}$ is calculated by

$$\widetilde{\mathbf{E}} = \boldsymbol{\gamma}_{(3)} [(\widetilde{\mathbf{B}} \odot \widetilde{\mathbf{A}})^T]^\dagger, \quad (30)$$

where the estimated factor matrices $\widetilde{\mathbf{A}}$ and $\widetilde{\mathbf{B}}$ can be reconstructed by the estimated AoAs/AoDs.

Then, a correlation-based scheme can be utilized to estimate the Doppler shifts as follows

$$\widetilde{f}_l = \arg \max_{f_l} \frac{|\overline{\mathbf{e}}_l^H \boldsymbol{\beta}(f_l)|}{\|\overline{\mathbf{e}}_l\|_2 \|\boldsymbol{\beta}(f_l)\|_2}, \quad 1 \leq l \leq J, \quad \widetilde{f}_l \in [0, f^{\max}], \quad (31)$$

where $\overline{\mathbf{e}}_l$ denotes the l th column of $\widetilde{\mathbf{E}}$. Finally, the path gains can be estimated through a simple least square (LS) method, such as

$$\widetilde{a}_l = \boldsymbol{\beta}(f_l)^\dagger \overline{\mathbf{e}}_l, \quad 1 \leq l \leq \widetilde{L}, \quad (32)$$

Therefore, all the parameters of mmWave time-varying channel are obtained and the final channel can be recovered. Furthermore, the detail steps are listed in the Algorithm 1.

Algorithm 1 Two-Stage Channel Estimation Algorithm for Time-Varying mmWave MIMO Channels

Input: Received signals \mathbf{y} and $\boldsymbol{\gamma}$, precoding matrices \mathbf{f}_1 and \mathbf{f}_2 , combing matrices \mathbf{w}_1 and \mathbf{w}_2 , one-dimensional search number J , and error threshold ε .

Output: The estimated mmWave time-varying channel parameters \widetilde{L} , $\widetilde{\mathbf{a}}$, $\widetilde{\boldsymbol{\theta}}$, $\widetilde{\boldsymbol{\varphi}}$, \widetilde{f} .

- 1: Construct the measurement matrix Θ by (12).
 - 2: Estimate the AoAs/AoDs and \widetilde{L} by (22) and BOMP algorithm.
 - 3: Update the estimated factor matrices $\widetilde{\mathbf{B}}$ and $\widetilde{\mathbf{A}}$ according to (27) and (28).
 - 4: Calculate the factor matrices $\widetilde{\mathbf{E}}$ by (30).
 - 5: Estimate the Doppler shifts \widetilde{f} by (31).
 - 6: Estimate the path gains $\widetilde{\mathbf{a}}$ according to (32).
-

V. PROPOSED TENSOR DECOMPOSITION-BASED TIME-VARYING CHANNEL ESTIMATION ALGORITHMS

By exploiting the low-rank structure of the time-varying channel, the time-varying channel estimation problem seems to be able to be formulated as a simple low-rank tensor decomposition problem. However, the conventional tensor decomposition-based algorithms [13], [14] are only designed for static channels. For comparison with these conventional algorithms, in this section, we propose two simple extended algorithms based on the conventional tensor decomposition-based channel estimation algorithms [13], [14].

A. SIMPLY EXTENDED TENSOR DECOMPOSITION-BASED ALGORITHM

We first consider utilizing the similar dimensional expansion method in (24) to model the received time-varying data into

a three-dimensional tensor, such as

$$\mathbf{R}_s(t) = \mathbf{w}_s^H \mathbf{H}(t) \mathbf{f}_s + \mathbf{N}(t) \quad (33)$$

where the design of precoder \mathbf{w}_s and combiner \mathbf{f}_s is similar to (24). And then, the three factor matrix can be rewritten as

$$\bar{\mathbf{A}} = \mathbf{w}_s^H \mathbf{A} \in \mathbb{C}^{N_{RF} \times L} \quad (34)$$

$$\bar{\mathbf{B}} = \mathbf{f}_s^T \mathbf{B} \in \mathbb{C}^{N_s \times L} \quad (35)$$

$$\mathbf{C} = [\boldsymbol{\beta}_1 \cdots \boldsymbol{\beta}_L] \in \mathbb{C}^{M \times L} \quad (36)$$

where the three matrices $\{\mathbf{A}, \mathbf{B}, \mathbf{C}\}$ have been described in section III-A. Besides, it is well known that the uniqueness of CP decomposition can be guaranteed [27], if the Kruskal's condition [28] is satisfied, i.e.

$$k_{\bar{\mathbf{A}}} + k_{\bar{\mathbf{B}}} + k_{\mathbf{C}} \geq 2L + 2, \quad (37)$$

where $k_{\bar{\mathbf{A}}}$, $k_{\bar{\mathbf{B}}}$, and $k_{\mathbf{C}}$ are the k -rank of matrices \mathbf{A} , \mathbf{B} , and \mathbf{C} , respectively. Note that the k -rank of the similar factor matrices \mathbf{A} and \mathbf{C} have been proofed as follows [14]

$$k_{\bar{\mathbf{A}}} = \min(N_{RF}, L) \quad (38)$$

$$k_{\mathbf{C}} = \min(M, L). \quad (39)$$

Then, consider that the k -rank is always less than or equal to the matrix rank, the k -rank of matrix $\bar{\mathbf{B}}$ is given by

$$\begin{aligned} k_{\bar{\mathbf{B}}} &\leq \text{rank}(\bar{\mathbf{B}}) \\ &= \text{rank}(\mathbf{f}_s^T \mathbf{B}) \\ &\leq \min(\text{rank}(\mathbf{f}_s^T), \text{rank}(\mathbf{B})). \end{aligned} \quad (40)$$

Note that $\mathbf{f}_s^T = (\mathbf{f}_{MS} \mathbf{f}_{BS})^T = \mathbf{f}_{BS}^T \mathbf{f}_{MS}^T$, therefore the rank of matrix \mathbf{f}_s^T is obtained as

$$\begin{aligned} \text{rank}(\mathbf{f}_s^T) &= \text{rank}(\mathbf{f}_{BS}^T \mathbf{f}_{MS}^T) \\ &\leq \min(\text{rank}(\mathbf{f}_{BS}^T), \text{rank}(\mathbf{f}_{MS}^T)) \\ &= 1. \end{aligned} \quad (41)$$

Substituting (41) into (40) yields

$$k_{\bar{\mathbf{B}}} \leq \min(1, \text{rank}(\mathbf{B})) = 1. \quad (42)$$

Then based on (42), the Kruskal condition is not satisfied, i.e.

$$k_{\bar{\mathbf{A}}} + k_{\bar{\mathbf{B}}} + k_{\mathbf{C}} \stackrel{(a)}{=} 2L + 1 < 2L + 2, \quad (43)$$

where (a) comes from the fact that the L is usually small.

Therefore, it can be easily verified that the simple dimensional expansion method for conventional tensor decomposition-based algorithm can not be utilized to estimate the time-varying channel. And then, the uniqueness of tensor decomposition can be guaranteed by utilizing the following approximation [19]:

$$\rho_l(1) \approx \rho_l(2) \dots \rho_l(M_1), \quad \mathbf{H}(1) \approx \mathbf{H}(2) \dots \mathbf{H}(M_1), \quad (44)$$

where M_1 denotes the number of sub-frames. Hence, by assuming the time-varying channel remain constant in a sub-frame, the precoding matrix \mathbf{F} and combining matrix \mathbf{W} can

Algorithm 2 Tensor Decomposition-Based Channel Estimation Algorithm for Time-Varying mmWave MIMO Channels

Input: Received tensor τ and MS beamforming matrix \mathbf{F} , BS measurement matrix \mathbf{W} , L , I and ε .

Output: The estimated a, θ, φ, f_d .

- 1: **Initialize:** Generate random initial matrices $\tilde{\mathbf{A}}^{(1)} \in \mathbb{C}^{N_{RF} \times L}$, $\tilde{\mathbf{B}}^{(1)} \in \mathbb{C}^{M_1 \times L}$, $\tilde{\mathbf{C}}^{(1)} \in \mathbb{C}^{T \times L}$, $n = 1$.
- 2: **repeat**
- 3: $n = n + 1$;
- 4: $\tilde{\mathbf{A}}^{(n)} = \tau_{(1)}[(\tilde{\mathbf{C}}^{(n-1)} \odot \tilde{\mathbf{B}}^{(n-1)})^T]^\dagger$;
- 5: $\tilde{\mathbf{A}}^{(n)} = \tilde{\mathbf{A}}^{(n)}_{:,j} / \|\tilde{\mathbf{A}}^{(n)}_{:,j}\|_2$, $1 \leq j \leq L$
- 6: $\tilde{\mathbf{B}}^{(n)} = \tau_{(2)}[(\tilde{\mathbf{C}}^{(n-1)} \odot \tilde{\mathbf{A}}^{(n)})^T]^\dagger$;
- 7: $\tilde{\mathbf{B}}^{(n)} = \tilde{\mathbf{B}}^{(n)}_{:,j} / \|\tilde{\mathbf{B}}^{(n)}_{:,j}\|_2$, $1 \leq j \leq L$
- 8: $\tilde{\mathbf{C}}^{(n)} = \tau_{(3)}[(\tilde{\mathbf{B}}^{(n)} \odot \tilde{\mathbf{A}}^{(n)})^T]^\dagger$;
- 9: $\tau^{(n)} = [\tilde{\mathbf{A}}^{(n)}, \tilde{\mathbf{B}}^{(n)}, \tilde{\mathbf{C}}^{(n)}]$
- 10: **until** $\frac{\|\tau^{(n+1)} - \tau^{(n)}\|_F^2}{\|\tau^{(n)}\|_F^2} \leq \varepsilon$
- 11: **for** $1 \leq l \leq L$ **do**
- 12: $\tilde{\theta}_l = \arg \max_{\theta_i} \frac{|\tilde{\mathbf{a}}_l^H \vec{\alpha}_{BS}(\theta_i)|}{\|\tilde{\mathbf{a}}_l\|_2 \|\vec{\alpha}_{BS}(\theta_i)\|_2}$, $1 \leq i \leq J$, $\theta_i \in [0, 2\pi]$
- 13: $\tilde{\varphi}_l = \arg \max_{\varphi_i} \frac{|\tilde{\mathbf{b}}_l^H \vec{\alpha}_{MS}(\varphi_i)|}{\|\tilde{\mathbf{b}}_l\|_2 \|\vec{\alpha}_{MS}(\varphi_i)\|_2}$, $1 \leq i \leq J$, $\varphi_i \in [0, 2\pi]$
- 14: $\tilde{f}_d^l = \arg \max_{f_d^l} \frac{|\tilde{\mathbf{c}}_l^H \vec{\beta}(f_d^l)|}{\|\tilde{\mathbf{c}}_l\|_2 \|\vec{\beta}(f_d^l)\|_2}$, $1 \leq i \leq J$, $f_d^l \in [0, f_d^{\max}]$
- 15: $\tilde{\mathbf{g}}(\tilde{f}_d^l) = [e^{j2\pi \tilde{f}_d^l M_1 T_s} \dots e^{j2\pi \tilde{f}_d^l T M_1 T_s}]^T$
- 16: $\tilde{\mathbf{A}} = [\vec{\alpha}_{BS}(\tilde{\theta}_1) \dots \vec{\alpha}_{BS}(\tilde{\theta}_L)]$
- 17: $\tilde{\mathbf{B}} = [\vec{\alpha}_{MS}(\tilde{\varphi}_1) \dots \vec{\alpha}_{MS}(\tilde{\varphi}_L)]$
- 18: $\tilde{\mathbf{C}} = \tau_{(3)}[(\tilde{\mathbf{B}} \odot \tilde{\mathbf{A}})^T]^\dagger$
- 19: $[\tilde{a}_1 \dots \tilde{a}_L] = \text{diag}([\tilde{\mathbf{g}}(\tilde{f}_d^1) \dots \tilde{\mathbf{g}}(\tilde{f}_d^K)])^\dagger \tilde{\mathbf{C}}$

be designed [13] to guarantee the uniqueness of CP decomposition. For clarity, we summarize the simple extended tensor decomposition-based algorithm [14] in Algorithm 2.

B. IMPROVED TENSOR DECOMPOSITION-BASED ALGORITHM

As we hold the (44) to guarantee the uniqueness of the CP decomposition, the method may approximation the time dimension information of the received tensor. Thus, the Algorithm 2 can not accurately estimate the path gains and Doppler shifts of the mmWave time-varying channel. In this subsection, we propose a improved two-stage tensor decomposition-based algorithm to estimate the time-varying channel.

In the first stage, we utilize the steps 1- 13 of the Algorithm 2 to estimate the AoAs/AoDs. Note the AoAs/AoDs keep constant during a training frame, the approximation (44) retains accurate angular information.

Then, in the second stage, the MS sends M_2 pilot signals to estimate the time-varying channel. Furthermore, based on the estimated angles and (29), the Doppler shifts and path gains can be extracted by utilizing the steps 14-19 of the Algorithm 3. Finally, the detailed steps can be seen in the Algorithm 3.

Algorithm 3 Improved Tensor Decomposition-Based Channel Estimation Algorithm for Time-Varying mmWave MIMO Channels

Input: Received tensors $\boldsymbol{\tau}$ and $\boldsymbol{\eta}$, MS beamforming matrix \mathbf{f}_1 and \mathbf{f}_2 , BS measurement matrix \mathbf{W} , L , I and ε .
Output: The estimated a , θ , φ , f_d .

- 1: **Initialize:** Generate random initial matrices $\tilde{\mathbf{A}}^{(1)} \in \mathbb{C}^{N_{RF} \times L}$, $\tilde{\mathbf{B}}^{(1)} \in \mathbb{C}^{M_1 \times L}$, $\tilde{\mathbf{C}}^{(1)} \in \mathbb{C}^{T \times L}$, $n = 1$.
- 2: **repeat**
- 3: $n = n + 1$;
- 4: $\tilde{\mathbf{A}}^{(n)} = \boldsymbol{\tau}_{(1)}[(\tilde{\mathbf{C}}^{(n-1)} \odot \tilde{\mathbf{B}}^{(n-1)})^T]^\dagger$;
- 5: $\tilde{\mathbf{A}}^{(n)} = \tilde{\mathbf{A}}^{(n)}_{:,j} / \left\| \tilde{\mathbf{A}}^{(n)}_{:,j} \right\|_2$, $1 \leq j \leq L$
- 6: $\tilde{\mathbf{B}}^{(n)} = \boldsymbol{\tau}_{(2)}[(\tilde{\mathbf{X}}^{(n-1)} \odot \tilde{\mathbf{A}}^{(n)})^T]^\dagger$;
- 7: $\tilde{\mathbf{B}}^{(n)} = \tilde{\mathbf{B}}^{(n)}_{:,j} / \left\| \tilde{\mathbf{B}}^{(n)}_{:,j} \right\|_2$, $1 \leq j \leq L$
- 8: $\tilde{\mathbf{C}}^{(n)} = \boldsymbol{\tau}_{(3)}[(\tilde{\mathbf{B}}^{(n)} \odot \tilde{\mathbf{A}}^{(n)})^T]^\dagger$;
- 9: $\boldsymbol{\tau}^{(n)} = [\tilde{\mathbf{A}}^{(n)}, \tilde{\mathbf{B}}^{(n)}, \tilde{\mathbf{C}}^{(n)}]$
- 10: **until** $\frac{\|\boldsymbol{\tau}^{(n+1)} - \boldsymbol{\tau}^{(n)}\|_F^2}{\|\boldsymbol{\tau}^{(n)}\|_F^2} \leq \varepsilon$
- 11: **for** $1 \leq l \leq L$ **do**
- 12: $\tilde{\theta}_l = \arg \max_{\theta_l} \frac{\left| \tilde{\mathbf{a}}_l^H \tilde{\boldsymbol{\alpha}}_{BS(\theta_l)} \right|}{\|\tilde{\mathbf{a}}_l\|_2 \|\tilde{\boldsymbol{\alpha}}_{BS(\theta_l)}\|_2}$, $1 \leq i \leq J$, $\theta_i \in [0, 2\pi]$
- 13: $\tilde{\varphi}_l = \arg \max_{\varphi_l} \frac{\left| \tilde{\mathbf{b}}_l^H \tilde{\boldsymbol{\alpha}}_{MS(\varphi_l)} \right|}{\|\tilde{\mathbf{b}}_l\|_2 \|\tilde{\boldsymbol{\alpha}}_{MS(\varphi_l)}\|_2}$, $1 \leq i \leq J$, $\varphi_i \in [0, 2\pi]$
- 14: $\tilde{\mathbf{A}} = [\tilde{\boldsymbol{\alpha}}_{BS(\tilde{\theta}_1)} \cdots \tilde{\boldsymbol{\alpha}}_{BS(\tilde{\theta}_L)}]$
- 15: **Redefine** $\tilde{\boldsymbol{\alpha}}_{MS(\varphi_l)} \triangleq \mathbf{f}_2^T \boldsymbol{\alpha}_{MS}^*(\varphi_l)$
- 16: $\tilde{\mathbf{B}} = [\tilde{\boldsymbol{\alpha}}_{MS(\tilde{\varphi}_1)} \cdots \tilde{\boldsymbol{\alpha}}_{MS(\tilde{\varphi}_L)}]$
- 17: $\tilde{\mathbf{C}} = \boldsymbol{\eta}_{(3)}[(\tilde{\mathbf{B}} \odot \tilde{\mathbf{A}})^T]^\dagger$
- 18: **for** $1 \leq l \leq L$ **do**
- 19: $\tilde{f}_d^l = \arg \max_{f_d^l} \frac{\left| \tilde{\mathbf{c}}_l^H \boldsymbol{\beta}(f_d^l) \right|}{\|\tilde{\mathbf{c}}_l\|_2 \|\boldsymbol{\beta}(f_d^l)\|_2}$, $1 \leq i \leq J$, $f_d^i \in [0, f_d^{\max}]$
- 20: $\mathbf{g}(\tilde{f}_d^l) = [e^{j2\pi\tilde{f}_d^l M_1 T_s} \cdots e^{j2\pi\tilde{f}_d^l T_1 T_s}]^T$
- 21: $[\tilde{a}_1 \dots \tilde{a}_L] = \text{diag}([\mathbf{g}(\tilde{f}_d^1) \dots \mathbf{g}(\tilde{f}_d^K)])^\dagger \tilde{\mathbf{Z}}$

VI. PERFORMANCE ANALYSIS

In this section, we provide the CRLB of the proposed two-stage time-varying channel estimation scheme, and then give the computational complexity order of our scheme.

A. CRLB ANALYSIS

Different from the previous work [18] focused on the CRLB of the channel estimation algorithm under the static channel, we discuss the CRLB of the proposed channel scheme under the time-varying channel. We firstly consider the received time-varying data in the second stage of our proposed scheme can be modeled as a three-dimensional tensor $\boldsymbol{\gamma} \in \mathbb{C}^{N_{RF} \times N_s \times M_2}$, such as

$$\boldsymbol{\gamma} = \sum_{l=1}^L a_l \tilde{\boldsymbol{\alpha}}_{BS(\theta_l)} \circ \tilde{\boldsymbol{\alpha}}_{MS(\varphi_l)} \circ \boldsymbol{\beta}_l + \mathbf{N}, \quad (45)$$

where the unknown time-varying channel parameters $\{a_l, \theta_l, \varphi_l, f_l\}$ are contained in this tensor, and each entry of \mathbf{N} is i.i.d zero mean, circular symmetric Gaussian random noise, of variance σ^2 . Then, similar to [29], [30], to simplify

the CRLB derivation, the unknown complex parameter vector can be expressed as

$$\boldsymbol{\mu} = [\theta_1 \dots \theta_L \varphi_1 \dots \varphi_L f_1 \dots f_L a_1 \dots a_L]. \quad (46)$$

Finally, the CRLB of the channel parameter estimation in the received tensor is given as follows [14], [31]

$$\begin{aligned} \text{CRLB}(\boldsymbol{\mu}) &= \boldsymbol{\Omega}^{-1}(\boldsymbol{\mu}) \\ &= \mathbf{E}^{-1} \left\{ \left(\frac{\partial f(\boldsymbol{\mu})}{\partial \boldsymbol{\mu}} \right)^H \left(\frac{\partial f(\boldsymbol{\mu})}{\partial \boldsymbol{\mu}} \right) \right\}, \end{aligned} \quad (47)$$

where $\boldsymbol{\Omega}(\boldsymbol{\mu})$ denotes the complex Fisher information matrix (FIM) [32], and the log-likelihood function $f(\boldsymbol{\mu})$ can be expressed as

$$\begin{aligned} f(\boldsymbol{\mu}) &= -N_{RF}N_sM_2 \ln(\pi\sigma^2) - \frac{1}{\sigma^2} \left\| \boldsymbol{\gamma}_{(1)}^T - (\mathbf{C} \odot \tilde{\mathbf{B}}) \tilde{\mathbf{A}} \right\|_F^2 \\ &= -N_{RF}N_sM_2 \ln(\pi\sigma^2) - \frac{1}{\sigma^2} \left\| \boldsymbol{\gamma}_{(1)}^T - (\mathbf{C} \odot \tilde{\mathbf{A}}) \tilde{\mathbf{B}} \right\|_F^2 \\ &= -N_{RF}N_sM_2 \ln(\pi\sigma^2) - \frac{1}{\sigma^2} \left\| \boldsymbol{\gamma}_{(1)}^T - (\tilde{\mathbf{B}} \odot \tilde{\mathbf{A}}) \mathbf{C} \right\|_F^2. \end{aligned} \quad (48)$$

B. COMPUTATIONAL COMPLEXITY ANALYSIS

We now discuss the computational complexity order of the proposed two-stage channel estimation scheme in the next two parts:

For the stage of AoAs/AoDs estimation, the computational complexity of the revised BOMP algorithm [18] is $\mathcal{O}(R\tilde{L}M_T N_R G + R\tilde{L}M_1 G + I^2\tilde{L}^3 M_1)$, where R denotes the number of iterations in each inner loop, I is the basis expansion model (BEM) order, and G denotes the number of angle grids.

For the stage of path gains and Doppler shifts estimation, the major computational task of the proposed method is the one-dimensional search method in (31). Thus, the complexity order of the second stage scheme at each iteration is $\mathcal{O}(JM_2)$.

Then, the total complexity order of the two stages is $\mathcal{O}(R\tilde{L}N_T N_R G + R\tilde{L}M_1 G + I^2\tilde{L}^3 M_1 + JM_2)$. To avoid the power leakage problem, the number of angle grids G is always very large, such as $G \gg N_T N_R$. Besides, the number of estimated path \tilde{L} and the iteration number R are very small. In particular, the total number of iterations in the second stage is the estimated path \tilde{L} , so the main complexity order for the one-dimensional search can be ignored. Therefore, the final complexity order of the proposed two-stage scheme can be simplified as $\mathcal{O}(RN_T N_R G + RIM_1 G + I^2\tilde{L}^3 M_1)$.

VII. SIMULATION RESULTS

In this section, we show the performance improvement of our proposed two-stage mmWave time-varying channel algorithm over other algorithms. Here, we consider a mmWave massive MIMO system with hybrid precoding, where $M_T = 16$, $N_R = 64$, $N_{RF} = 6$. For the geometric mmWave channel parameters, the number of paths is set $L = 3$, the AoAs/AoDs are assumed to distribute in $[0, 2\pi]$, and the static complex

gain a_l follows a circularly symmetric Gaussian distribution. Furthermore, for the time-varying channel parameters, the Doppler shift f_l is randomly distributed in $[0, f^{\max}]$, $T_s = 1\mu s$, and the carrier frequency $f_c = 60$ GHz. In Algorithm 1, we take $J = 600$ and $N_s = 32$ to get a better tradeoff between the performance and complexity order. Besides, the total transmission time instant of our method is $M_p = M_1 + M_2$, where $M_1 = 120$, $M_2 = 30$.

To examine the estimation performance of the time-varying channel parameters $\{a, \theta, \varphi, f\}$, in this section, the mean square error (MSE) is utilized to evaluate the estimation accuracy separately, such as

$$MSE(\mathbf{x}) = E \left[\|\mathbf{x} - \tilde{\mathbf{x}}\|_2^2 \right], \quad (49)$$

where \mathbf{x} and $\tilde{\mathbf{x}}$ denote the real parameter vector and estimated parameter vector, respectively. Then, the normalized mean square error (NMSE) is utilized to examine the estimation accuracy of the time-varying channel, such as

$$NMSE = 10\log_{10} \left(E \left[\frac{\|\mathbf{H} - \tilde{\mathbf{H}}\|_F^2}{\|\mathbf{H}\|_F^2} \right] \right), \quad (50)$$

where $\tilde{\mathbf{H}}$ denotes the estimated time-varying channel.

A. ESTIMATION PERFORMANCE OF THE TIME-VARYING CHANNEL PARAMETERS

In this subsection, the estimation accuracy of our proposed two-stage method is compared with the conventional tensor decomposition-based mmWave channel estimation methods Algorithm 2 and Algorithm 3, which are proposed in Section V.

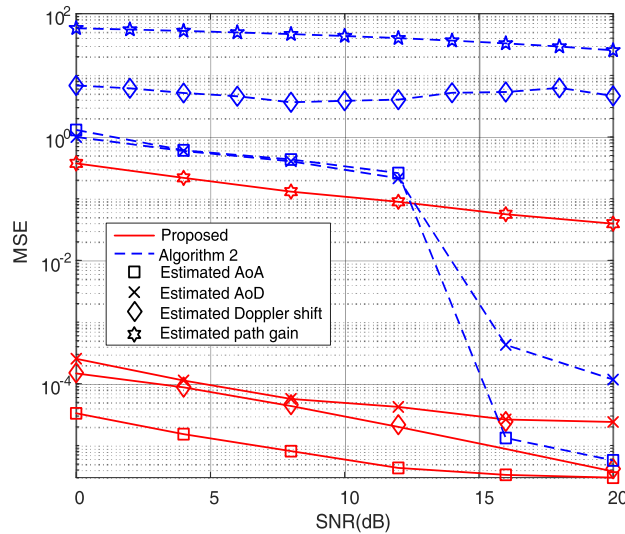


FIGURE 3. MSEs comparison among the proposed method and the Algorithm 2 versus SNR, $v = 120$ km/h.

Fig. 3 plots the MSEs performance versus signal-to-noise (SNR) of our proposed two-stage method and the simply extended CP decomposition-based method (Algorithm 2).

From Fig. 3, it is clear to see that the proposed method can accurately estimate all parameters of the mmWave time-varying channel, in the meantime, the conventional CP based method may not. The reason for this phenomenon may be that the conventional method needs to guarantee the uniqueness of decomposition, which blurs the information in the time dimension. Furthermore, by utilizing the block-sparsity of time-varying channel, the proposed scheme achieves a better estimation accuracy for angle estimation even under low SNR compared with the conventional CP method.

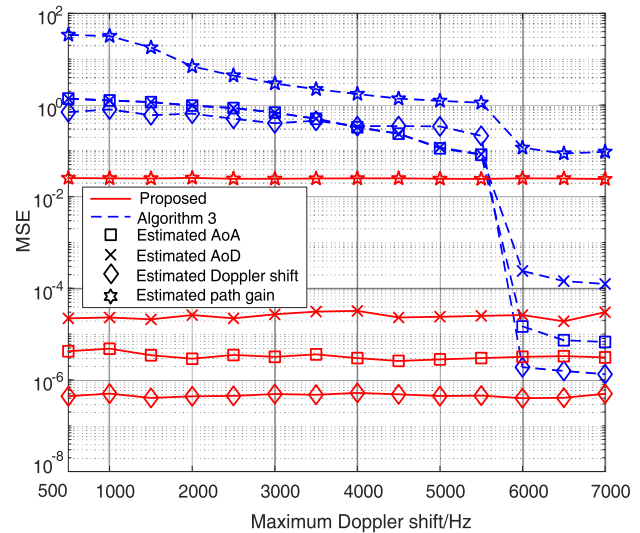


FIGURE 4. MSEs comparison among the proposed method and the Algorithm 3 versus the maximum doppler shift, SNR = 20dB.

Considering the problem of conventional tensor decomposition based algorithm in estimating time-varying channels, we proposed a improved algorithm (Algorithm 3) in the Section V-B. Then, in Fig. (4) and Fig. (5), we examine the channel parameter estimation performance of the proposed two-stage method and the Algorithm 3.

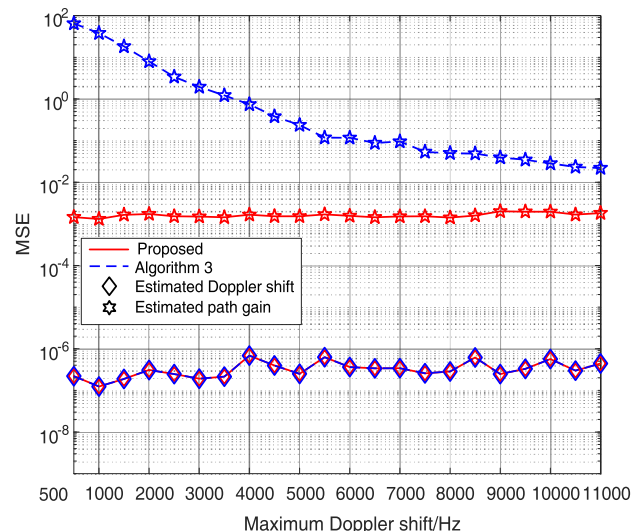


FIGURE 5. MSEs comparison versus the maximum doppler shift with priori knowledge of AoAs/AoDs, SNR = 20dB.

Firstly, Fig. (4) portrays the MSEs performance comparison of the different algorithms versus the maximum Doppler shift with SNR = 20dB. Observed from Fig. (4) that, for the high maximum Doppler shift, the proposed improved algorithm obtains a good MSE performance for all the time-varying channel parameters. This implies that the improved tensor decomposition-based algorithm can effectively extract time dimension information from the received data when the maximum Doppler shift is high. However, when the maximum Doppler shift is low, the improved algorithm performs poorly due to the fact that the uniqueness condition of the CP decomposition no longer exists. It's also shown that the propose two-stage method are robust to different Doppler shifts. This is because that our method utilize the joint block-sparse and low-rank structures of the mmWave time-varying channel.

Secondly, in order to investigate the estimation performance without considering the uniqueness condition of the CP decomposition, we depict the MSEs curves against the maximum Doppler shift based on the ideal AoAs/AoDs in Fig. (5). From Fig. (5), we see that the improved tensor decomposition-based algorithm still performs poorly when estimating the path gains for the low maximum Doppler shift, even with the ideal AoAs/AoDs. This indicates that the proposed LS path gain estimation is superior to the method in the Algorithm 3.

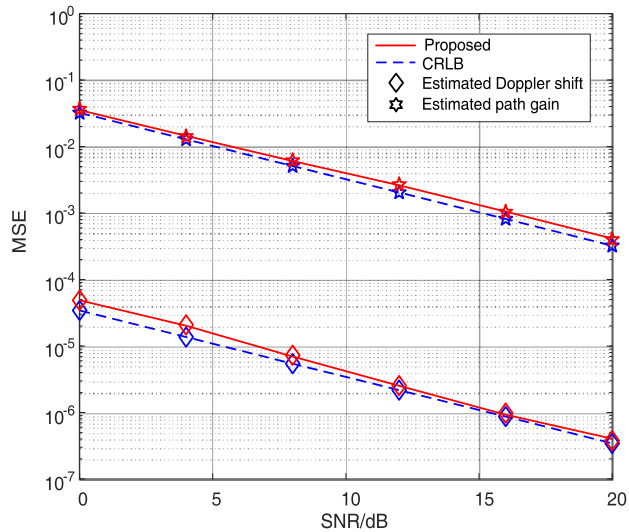


FIGURE 6. MSEs and CRLBs of the proposed method versus SNR with prior knowledge of AoAs/AoDs, $v = 120$ km/h.

Finally, as analyze in the Section VI-A, the theoretical CRLB derived in (47) is provided as the benchmark. Then, Fig. (6) compares the MSEs performance of the proposed two-stage method and the CRLBs with the prior knowledge of AoAs/AoDs. As can be observed from Fig. (6), the MSEs performance attained by our proposed two-stage method are close to their corresponding CRLBs, even in the low SNR region.

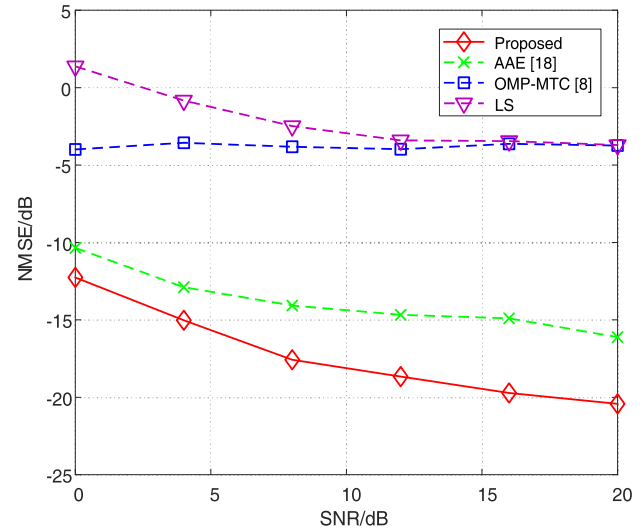


FIGURE 7. NMSE comparison among the different algorithms versus SNR, $v = 120$ km/h.

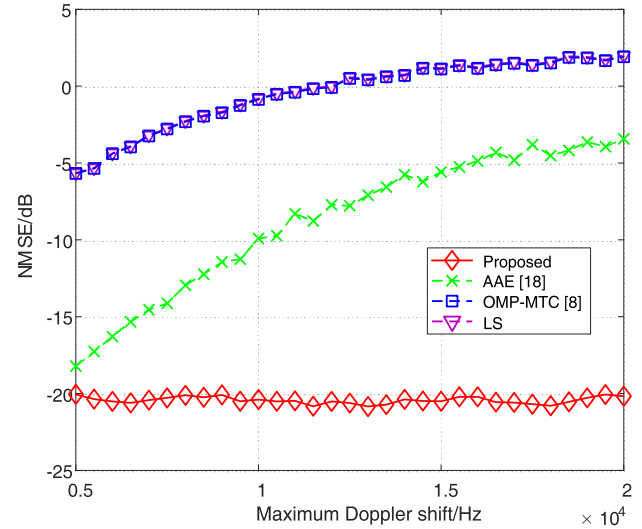


FIGURE 8. NMSE comparison among the different algorithms versus the maximum Doppler shift, SNR = 20dB.

B. ESTIMATION PERFORMANCE OF THE TIME-VARYING CHANNEL

In this subsection, the performance of our proposed scheme is compared with other conventional algorithms, such as the OMP-minimal total coherence (OMP-MTC) algorithm [8], the LS algorithm and the revised AAE algorithm [18]. In particular, the AAE algorithm is designed based on the time-varying channel, which makes use of the block-sparsity characteristic. Furthermore, the total numbers of pilots in LS, OMP-MTC, AAE are 1024, 1024, 130, respectively.

In Fig. 7, we show the time-varying channel estimation performance of different schemes versus SNR. As expected, the AAE algorithm obtains a good performance, while it still have some performance loss compared with our proposed algorithm. The above phenomenon may be due to the joint block-sparse and low-rank characteristic is utilized in our proposed algorithm. Then, in Fig. 8, we examine the performance

of different algorithms as a function of the maximum Doppler shift from 5kHz to 20kHz, with the corresponding velocities from 90km/h to 360km/h. Obviously, the AAE algorithm lacks robustness when the maximum Doppler shift is very high. It is important to point that, our proposed scheme maintains a stable and better estimation performance with the increase of Doppler shift, compared with other algorithms. This is due to the fact that our proposed algorithm captures the channel information in the time dimension, by utilizing the low-rank structure of the received three-order tensor.

VIII. CONCLUSION

In this paper, the problem of time-varying channel estimation for mmWave systems with hybrid structures is studied. In particular, it is shown that the block sparsity, along with the low-rank structure, can be utilized to extract the Doppler shifts and other channel parameters. Thus, a two-stage channel estimation method is developed, in which the block-sparsity is utilized to estimate the AoAs/AoDs, and then followed by a tensor decomposition-based method to extract the path gains and the Doppler shifts based on the estimated AoAs/AoDs. Moreover, in order to compare with conventional tensor decomposition-based channel estimation algorithms, two simple extended algorithms for time-varying channel estimation are proposed. Simulation results demonstrate that the proposed scheme outperforms the conventional compressed sensing-based algorithms and the tensor decomposition-based algorithms. Moreover, simulation results also show that the proposed scheme remains close to the CRLBs even in the low SNR region with the priori knowledge of AoAs/AoDs.

REFERENCES

- [1] F. Boccardi, R. W. Heath, Jr., A. Lozano, T. L. Marzetta, and P. Popovski, "Five disruptive technology directions for 5G," *IEEE Commun. Mag.*, vol. 52, no. 2, pp. 74–80, Feb. 2014.
- [2] T. S. Rappaport, S. Sun, R. Mayzus, H. Zhao, Y. Azar, K. Wang, G. N. Wong, J. K. Schulz, M. Samimi, and F. Gutierrez, "Millimeter wave mobile communications for 5G cellular: It will work!" *IEEE Access*, vol. 1, pp. 335–349, May 2013.
- [3] X. Gao, L. Dai, and A. M. Sayeed, "Low RF-complexity technologies to enable millimeter-wave MIMO with large antenna array for 5G wireless communications," *IEEE Commun. Mag.*, vol. 56, no. 4, pp. 211–217, Apr. 2018.
- [4] P. Zhou, K. Cheng, X. Han, X. Fang, Y. Fang, R. He, Y. Long, and Y. Liu, "IEEE 802.11ay-based mmWave WLANs: Design challenges and solutions," *IEEE Commun. Surveys Tuts.*, vol. 20, no. 3, pp. 1654–1681, 3rd Quart., 2018.
- [5] Z. Pi, J. Choi, and R. W. Heath, Jr., "Millimeter-wave gigabit broadband evolution toward 5G: Fixed access and backhaul," *IEEE Commun. Mag.*, vol. 54, no. 4, pp. 138–144, Apr. 2016.
- [6] S. Kutty and D. Sen, "Beamforming for millimeter wave communications: An inclusive survey," *IEEE Commun. Surveys Tuts.*, vol. 18, no. 2, pp. 949–973, 2nd Quart., 2016.
- [7] A. Alkhateeb, O. El Ayach, G. Leus, and R. W. Heath, Jr., "Channel estimation and hybrid precoding for millimeter wave cellular systems," *IEEE J. Sel. Topics Signal Process.*, vol. 8, no. 5, pp. 831–846, Oct. 2014.
- [8] J. Lee, G.-T. Gil, and Y. H. Lee, "Channel estimation via orthogonal matching pursuit for hybrid MIMO systems in millimeter wave communications," *IEEE Trans. Commun.*, vol. 64, no. 6, pp. 2370–2386, Jun. 2016.
- [9] X. Li, J. Fang, H. Li, and P. Wang, "Millimeter wave channel estimation via exploiting joint sparse and low-rank structures," *IEEE Trans. Wireless Commun.*, vol. 17, no. 2, pp. 1123–1133, Feb. 2018.
- [10] C. Hu, L. Dai, T. Mir, Z. Gao, and J. Fang, "Super-resolution channel estimation for mmWave massive MIMO with hybrid precoding," *IEEE Trans. Veh. Technol.*, vol. 67, no. 9, pp. 8954–8958, Sep. 2018.
- [11] Z. Gao, C. Hu, L. Dai, and Z. Wang, "Channel estimation for millimeter-wave massive MIMO with hybrid precoding over frequency-selective fading channels," *IEEE Commun. Lett.*, vol. 20, no. 6, pp. 1259–1262, Jun. 2016.
- [12] J. Rodríguez-Fernández, K. Venugopal, N. González-Prelcic, and R. W. Heath, Jr., "A frequency-domain approach to wideband channel estimation in millimeter wave systems," in *Proc. IEEE Int. Conf. Commun. (ICC)*, May 2017, pp. 1–7.
- [13] Z. Zhou, J. Fang, L. Yang, H. Li, Z. Chen, and S. Li, "Channel estimation for millimeter-wave multiuser MIMO systems via PARAFAC decomposition," *IEEE Trans. Wireless Commun.*, vol. 15, no. 11, pp. 7501–7516, Nov. 2016.
- [14] Z. Zhou, J. Fang, L. Yang, H. Li, Z. Chen, and R. S. Blum, "Low-rank tensor decomposition-aided channel estimation for millimeter wave MIMO-OFDM systems," *IEEE J. Sel. Areas Commun.*, vol. 35, no. 7, pp. 1524–1538, Jul. 2017.
- [15] F. J. Martín-Vega, M. C. Aguayo-Torres, G. Gomez, J. T. Entrambasagras, and T. Q. Duong, "Key technologies, modeling approaches, and challenges for millimeter-wave vehicular communications," *IEEE Commun. Mag.*, vol. 56, no. 10, pp. 28–35, Oct. 2018.
- [16] Z. Xiao, P. Xia, and X.-G. Xia, "Enabling UAV cellular with millimeter-wave communication: Potentials and approaches," *IEEE Commun. Mag.*, vol. 54, no. 5, pp. 66–73, May 2016.
- [17] H. Song, X. Fang, and Y. Fang, "Millimeter-wave network architectures for future high-speed railway communications: Challenges and solutions," *IEEE Wireless Commun.*, vol. 23, no. 6, pp. 114–122, Dec. 2016.
- [18] Q. Qin, G. Lin, P. Cheng, and B. Gong, "Time-varying channel estimation for millimeter wave multiuser MIMO systems," *IEEE Trans. Veh. Technol.*, vol. 67, no. 10, pp. 9435–9448, Oct. 2018.
- [19] N. Aboutorab, W. Hardjawana, and B. Vucetic, "Application of compressive sensing to channel estimation of high mobility OFDM systems," in *Proc. IEEE Int. Conf. Commun. (ICC)*, Jun. 2013, pp. 4946–4950.
- [20] J. Rodríguez-Fernández, N. González-Prelcic, K. Venugopal, and R. W. Heath, Jr., "Frequency-domain compressive channel estimation for frequency-selective hybrid millimeter wave MIMO systems," *IEEE Trans. Wireless Commun.*, vol. 17, no. 5, pp. 2946–2960, May 2018.
- [21] W. U. Bajwa, J. Haupt, A. M. Sayeed, and R. Nowak, "Compressed channel sensing: A new approach to estimating sparse multipath channels," *Proc. IEEE*, vol. 98, no. 6, pp. 1058–1076, Jun. 2010.
- [22] S. Rangan, T. S. Rappaport, and E. Erkip, "Millimeter-wave cellular wireless networks: Potentials and challenges," *Proc. IEEE*, vol. 102, no. 3, pp. 366–385, Mar. 2014.
- [23] Q. Qin, L. Gui, B. Gong, J. Xiong, and X. Zhang, "Compressive sensing based time-varying channel estimation for millimeter wave systems," in *Proc. IEEE Int. Symp. Broadband Multimedia Syst. Broadcast. (BMSB)*, Jun. 2017, pp. 1–6.
- [24] J. A. Tropp and A. C. Gilbert, "Signal recovery from random measurements via orthogonal matching pursuit," *IEEE Trans. Inf. Theory*, vol. 53, no. 12, pp. 4655–4666, Dec. 2007.
- [25] Y. C. Eldar, P. Kuppinger, and H. Boche, "Block-sparse signals: Uncertainty relations and efficient recovery," *IEEE Trans. Signal Process.*, vol. 58, no. 6, pp. 3042–3054, Jun. 2010.
- [26] B. Xu, Y. Zhao, Z. Cheng, and H. Li, "A novel unitary PARAFAC method for DOD and DOA estimation in bistatic MIMO radar," *Signal Process.*, vol. 138, pp. 273–279, Sep. 2017.
- [27] T. G. Kolda and B. W. Bader, "Tensor decompositions and applications," *SIAM Rev.*, vol. 51, no. 3, pp. 455–500, Aug. 2009.
- [28] A. Stegeman and N. D. Sidiropoulos, "On Kruskal's uniqueness condition for the candecomp/parafac decomposition," *Linear Algebra Appl.*, vol. 420, nos. 2–3, pp. 540–552, Jun. 2007.
- [29] A. Van Den Bos, "A Cramer-Rao lower bound for complex parameters," *IEEE Trans. Signal Process.*, vol. 42, no. 10, p. 2859, Oct. 1994.
- [30] S. F. Yau and Y. Bresler, "A compact Cramér-Rao bound expression for parametric estimation of superimposed signals," *IEEE Trans. Signal Process.*, vol. 40, no. 5, pp. 1226–1229, May 1992.
- [31] X. Liu and N. D. Sidiropoulos, "Cramér-Rao lower bounds for low-rank decomposition of multidimensional arrays," *IEEE Trans. Signal Process.*, vol. 49, no. 9, pp. 2074–2086, Sep. 2001.
- [32] S. M. Kay, *Fundamentals of Statistical Signal Processing: Estimation Theory*. Upper Saddle River, NJ, USA: Prentice-Hall, 1993.



LONG CHENG was born in Kaifeng. He received the B.E. degree in communication and information system from the University of Electronic Science and Technology of China, in 2016, where he is currently pursuing the Ph.D. degree with the National Key Laboratory of Science and Technology on Communications. He is also an Engineer with the Science and Technology on Information Transmission and Dissemination in Communication Networks Laboratory. His current research interests include millimeter-wave communications and high speed railway communications.



YUEYUE LIANG was born in Sichuan. She received the bachelor's degree from Beijing University of Posts and Telecommunications.



GUANGRONG YUE received the Ph.D. degree in communication and information system from the University of Electronic Science and Technology of China (UESTC), Chengdu, China, in 2006. He was a Postdoctoral Fellow with the Department of Electrical Engineering and Computer Science, University of California at Berkeley, Berkeley, CA, USA, from 2007 to 2008. He has been a Faculty Member in telecommunications engineering with UESTC, since 2008. His major research interests include wireless communication theory, short range communications, and adaptive signal processing.



DAIZHONG YU received the B.S. degree from the University of Electronic Science and Technology of China (UESTC), Chengdu, China, in 2016, and the master's degree from the National Key Laboratory of Communication, UESTC. His current research interests include measurement and modeling of wireless propagation channels, high-speed railway communications, and millimeter-wave (mmWave) communication systems.



SHAOQIAN LI (F'16) received the B.S.E. degree in communication technology from the Northwest Institute of Telecommunication, Xidian University, in 1982, and the M.S.E. degree in communication system from the University of Electronic Science and Technology of China (UESTC), in 1984, where he is currently a Professor, a Ph.D. Supervisor, and the Director of the National Key Laboratory of Science and Technology on Communications. He is also a member of the National High Technology Research and Development Program (863 Program) Communications Group. His research interests include wireless communication theory, anti-interference technology for wireless communications, spread-spectrum and frequency hopping technology, and mobile and personal communications.

• • •